Structures 67 (2024) 106974

Contents lists available at ScienceDirect

Structures

journal homepage: www.elsevier.com/locate/structures

Synergistic effect of rice husk ash and ceramic powder on mechanical properties of ultra-high-performance concrete

Hoang TMK Trinh [a], Paththini HHU Fernando [b], Tung M. Tran [a], Thong M. Pham [c,*]

[a] Sustainable Developments in Civil Engineering Research Group, Faculty of Civil Engineering, Ton Duc Thang University, Ho Chi Minh City, Viet Nam
[b] CPB Contractors, 202 Pier Street, Perth, WA 6000, Australia
[c] UniSA STEM, University of South Australia, Mawson Lakes, SA 5095, Australia

ARTICLE INFO

Keywords:
Ultra-high performance concrete (UHPC)
Rice husk ash (RHA)
Ceramic powder (CP)
Mechanical properties
Damping ratio
Environmental impact assessment
Cost analysis

ABSTRACT

This research examines the synergistic impacts of incorporating rice husk ash (RHA) and ceramic powder (CP) in ultra-high-performance concrete (UHPC). Four alternatives of UHPCs with different contents of RHA and CP were investigated. Specifically, the first two batches substituted silica fume (SF) with RHA at levels of 5 %, 10 %, and 15 %, whereas 10 %, 15 %, and 20 % RHA was used to replace cement in the third batch. The last batch, on the other hand, was designed to examine the synergistic effect of a fixed 5 % RHA and CP replacement proportions of 10 %, 15 %, and 20 %. Mechanical properties (i.e. compressive/flexural resistance and damping ratio), economic efficiency, and environmental impacts of the newly designed mixtures were determined. Compared to the reference mix, all mixtures experienced declined workability. While using RHA to replace SF exhibited either comparable or enhanced compressive and bending capacities, mixes with cement substitution had lower compressive strengths but higher flexural strengths. Regardless of substituting cement or SF, incorporating RHA consistently augmented the damping performance of the UHPC blends. The inclusion of both RHA and CP resulted in up to 17.2 % higher compressive strength, 47.9–59.1 % higher flexural strength, and 68 % higher damping ratio compared to the control mix, highlighting their favourable synergistic effects for developing high-performance and eco-friendly UHPC mixtures. The developed mixtures also demonstrated improvements of up to 40 % in cost-efficiency and reductions of up to 10.1 % in embodied carbon emissions (38 % carbon index).

1. Introduction

The current increasing demand for housing and infrastructure has caused a soar in global production rates of concrete, leading to its being the most commonly used construction materials. In recent years, there have been notable advancements in concrete technology, including the development of ultra-high performance concrete (UHPC), which is a type of concrete that can boost the compressive capacity to over 150 MPa and the tensile strength of up to 15 MPa [1]. Moreover, UHPC possesses good workability, high toughness, and excellent resistance to long-term creep, freeze-thaw cycles, and salt-scaling [1,2]. A typical mix of UHPC contains high cement content of 900–1000 kg/m^3, silica fume (SF) of 150–250 kg/m^3, quartz powder and quartz sand [1,2]. Steel fibres are also added to improve the UHPC's ductility, flexural strength, and dispense the need for passive reinforcement in some instances [3]. Given these remarkable mechanical and durable properties, UHPC provides a propitious solution to lighter and eco-friendlier structures with longer service life, less material consumption and higher structural efficiency in comparison with using conventional concrete and other building materials [3,4].

The cement industry has been identified as one of the largest environment defilers, accounting for 5–7 % of the global carbon emissions [5]. Since an UHPC mix usually requires a great amount of cement, mitigating CO_2 emissions released in the manufacture of UHPC is of great importance. To achieve "green" concrete, material scientists have been focusing on utilising supplementary cementitious materials (SCMs) to reduce the dependence on cement, achieving different levels of accomplishment [6–8]. Ground granulated blast furnace slag (GGBFS), fly ash (FA), and silica fume (SF) are the most common SCMs [5]. Despite their widespread usage in replacing cement in the production of

* Corresponding author.
E-mail addresses: trinhtranmaikimhoang@tdtu.edu.vn (H.T. Trinh), hivin.fernando@newest-wa.com.au (P.H. Fernando), tranminhtung@tdtu.edu.vn (T.M. Tran), thong.pham@unisa.edu.au (T.M. Pham).

https://doi.org/10.1016/j.istruc.2024.106974
Received 7 May 2024; Received in revised form 1 July 2024; Accepted 19 July 2024
Available online 2 August 2024

UHPC, they are not deemed as effective and sustainable alternatives. This is because they are by-products of energy-intensive and polluting industrial processes. In fact, the amount of FA has been reduced in North America since coal-fired power plants are being transformed to gas-fired plants; and the production cost of SF is substantial due to the scarcity of resources [5]. Another issue is that transporting these by-products from distant locations can discharge a massive amount of carbon emissions to the atmosphere. Therefore, using local recycled waste materials is becoming a preferred practice [9].

Worldwide, an annual production of approximately 160 million tons of rice husk from rice paddies raises significant environmental concerns in rice-producing countries [10]. On the one hand, disposing of these husks in landfills consumes extensive space, leading to potential land shortages. On the other hand, incineration leads to the generation of ashes, posing a threat to air quality and the aesthetic appeal of surrounding areas. Even the fermentation of rice husk by microorganisms results in the emission of methane, a greenhouse gas contributing to global warming [11]. Controlled burning rice husks at temperature between 600–850 °C produces a solid residue known as rice husk ash (RHA) [12]. With a high SiO_2 content of 90–96 % and an extremely fine texture, this RHA is considered a promising SCM [13]. RHA, similar to SF and FA, are classified as highly pozzolanic materials. The presence of RHA improves the hydration process and the microstructure of the cement paste [14]. Specifically, RHA can decrease the concrete mixture's porosity, the $Ca(OH)_2$ content in the interfacial transition zone (ITZ) between cement paste and aggregates, and the width of the ITZ [14]. Due to these beneficial characteristics, RHA have been reported to positively contribute to concrete mechanical properties and durability [12,13,15–21], allowing for its partial/full substitution for conventional cementitious materials. Besides, considering its related environmental issues and the increasing shortage of other SCMs, RHA provides an economical, advantageous, and sustainable alternative for conventional binders, especially in agricultural countries where rice husk is vastly accessible from rice production.

Previous studies have been carried out to investigate the optimal replacement proportions of RHA for concrete and/or SF in many genres of concrete, including UHPC [3,15,17,18,20–24]. A cement replacement ratio of 5–30 % with RHA was documented to improve hardened properties of concrete mixes. For normal concrete, Gastaldini et al. [21] found a mixture having 20 % RHA and 1 % K_2SO_4 (by weight of cement) as a chemical activator possessed higher compressive strength than that of the control mix. Specifically, at 91 days old, the increase in compressive strength was up to 43 % [21]. Similar outcomes were reported by Chindaprasirt et al. [20]. Moreover, Saraswathy and Song [22] discovered that the addition of RHA of up 30 % dosage diminished the permeability and chloride penetration of the concrete paste, leading to enhanced corrosion resistance and strength. Regarding high performance concrete (HPC), Cordeiro et al. [23] found ultrafine RHA having particle size of 3 μm enhanced the mechanical behaviour and durability of HPC blends, particularly for 20 % replacement. At the same time, Salas et al. [15] stated that the use of 5–10 % RHA enhanced the compressive capacity and exhibited comparable strength with HPC paste having the same amount of SF. In a research on self-consolidating high performance concrete (SHPC), Safiuddin et al. [24] observed that RHA-based mixtures obtained higher compressive strengths than that of the control mix, especially for longer curing days. Accordingly, the authors found 15 % replacement of RHA was the optimum proportion for SHPC, having outstanding strengths and acceptable workability [24].

Considering UHPC, Nguyen et al. [18] reported that the compressive strength of RHA-incorporated specimen surpassed that of the reference sample, even after three and seven days. Likewise, Huang et al. [17] documented that 2/3 substitution dosage of RHA for SF significantly increased the compressive strength of UHPCs, by 14.5 % at 28 days. Compared to the control specimen, reactive powder concrete (RPC), a type of UHPC, showed significant improvements in compressive and flexural strengths, with increments of up to 56 % and 44 %, respectively [13]. In addition, the 30 % RHA-added mixture exhibited greater compressive, splitting tensile and flexural resistance than other mixes, being the optimum percentage [13]. Apart from augmented hardened properties, RHA was found to delay and decelerate the self-desiccation of UHPCs, addressing the problematic autogenous shrinkage [16,25]. In summary, existing research has consistently demonstrated that the optimum cement/SF replacement by RHA falls between 10 % and 30 %, depending on several factors.

According to Ray et al. [26], the production of concrete requires 1.5 billion tons of cement, 10–20 billion tons of aggregates, and about 1 billion tons of water per year. With the increasing global population, it is anticipated that the demand for concrete will reach approximately 18 billion tons per year [26]. Such high demand for local natural resources in concrete production will evidently have negative impacts on the natural environment, including erosion of river deltas and coastlines due to the extraction of natural sand and gravel [26]. To address this issue, the use of substitute materials as a replacement for natural aggregates (NA) has been recommended and gained more attendance. At present, the use of ceramic as a furnishing material is very popular. However, once ceramic reaches the end of its lifespan, it loses its value and becomes mere waste. According to Mukhopadhyay et al. [27], around 50, 000 tonnes of ceramic waste (CW) is generated each year. Similar to other forms of waste, the accumulation of CW is increasing day by day and creating a burden for the ceramic industry, necessitating a viable solution for its disposal. According to Halicka et al. [28], ceramic aggregates (CA) exhibit resistance to abrasion and heat, and possess a low thermal expansion coefficient. Additionally, ceramic products are characterised by high strength, wear and fire resistance, chemical inertness, and longevity [29]. Therefore, utilising CW as a substitute for NA could be an effective and promising practice for both concrete production and waste management industry.

Previous researchers have investigated the properties of CA along with the mechanical properties of CA-based concrete [28–34]. According to Guerra et al. [31] concrete samples containing 5 %, 7 %, and 9 % recycled coarse CA exhibited comparable compressive capacity at all curing ages, in comparison with the control concrete sample. Likewise, Medina et al. [29] discovered that the incorporation of recycled coarse sanitary ware CA in concrete mixes led to an increase in compressive and splitting tensile strengths. This could be due to the more compact microstructure in the ITZ between the recycled CA and paste compared to that between NA and paste. Positive findings were also presented in [32], in which recycled CA concrete attained 24.74 % higher compressive strength and 34.25 % higher tensile strength than that of ultra-high strength concrete made of gravel-basalt aggregates. Kannan et al. [33] performed mechanical, durability, and microstructural tests on HPC mixtures having 10–40 % ceramic powder (CP) as substitution of cement. Compared to the reference mixture, the resulting HPCs obtained lower compressive strength at early age, yet comparable compressive strength at later age. Durability and electrical resistivity of the examined mixtures were significantly improved with the addition of CP. In like manner, Xu et al. [34] investigated the mechanical properties and carbon efficiency of UHPC incorporating tile-waste CP. From the results, the adopted CP was shown highly pozzolanic that enhanced the hydration degree and decreased the ITZ and total porosity of the cement paste. In addition, the inclusion of 55 % tile-waste CP in UHPCs led to reductions in energy demand, carbon footprint, and material cost by 41.0 %, 33.1 %, and 25.9 %, respectively.

While the advantageous influence of CP has been shown, optimal substitution proportions of NA with CP has not been clearly determined. Although studies have shown the advantages of concrete incorporated with RHA and CP, limited research has scrutinised their collective effects on concrete mechanical characteristics. Therefore, this research was to investigate the use of RHA and CP in the development of an innovative, less expensive, and environmentally friendly UHPC. The effects of RHA and CP on the rheological properties, compressive and flexural capacities, damping ratios of UHPC, along with production cost and

environmental impact, were investigated. Accordingly, a two-stage experimental programme was performed, including four batches and twelve mix designs of UHPC. Specifically, Stage 1 examined the partial replacement of SF with RHA for two different portions of steel fibres in batches B1 and B2 and the substitution of cement with RHA in batch B3. After identifying the best performing mix design in Stage 1, Stage 2 was conducted to inspect the synthesised effects of simultaneously replacing SF with RHA and SS with CP, while keeping a constant replacement ratio of RHA.

2. Experimental programme

This section describes the material features, mixture proportions, mix-design optimisation, specimen preparation and test methods.

2.1. Rationale of the mix design

In this study, RHA and CP were combined as supplementary cementitious materials for UHPC. The rationale behind this specific combination was to investigate the potential synergistic effects of incorporating these two waste materials simultaneously. RHA is a highly pozzolanic by-product from the rice industry, while CP is obtained by pulverising ceramic waste from construction and demolition activities. By combining RHA and CP, the study aimed to explore if their individual benefits on concrete properties could be enhanced through synergistic interactions, leading to improved mechanical performance and sustainability of UHPC mixtures.

Since SF is a commonly used SCM and well-known for enhancing the mechanical properties and durability of UHPC, it was also incorporated in the UHPC mixtures. The inclusion of SF served as a reference point to compare the performance of RHA and CP against a well-established pozzolanic admixture. By partially substituting SF with RHA in some mixtures and maintaining SF in others, the study aimed to evaluate the efficacy of RHA as a potential alternative to SF. This approach allowed for a comprehensive assessment of the synergistic effects between RHA, CP, and SF in developing high-performance and sustainable UHPC mixtures.

2.2. Materials

This experiment used a general purpose type cement, which is compliant with all regulations and stipulations outlined in AS 3972–2010 – General purpose and blended cements [35]. Cement had 10–30 % particle size of 7 μm and a bulk density of 1000 kg/m^3. Along with cement, SF and RHA also act as binders. The added SF had a median particle size of approximately 0.5 μm and specific gravity (SG) of 2.2–2.3. The utilised RHA, as illustrated in Fig. 1, was supplied by Xetex Industries Pvt. Ltd, India. The median particle size of RHA was 25 μm with SG of 2.18. The chemical composition of RHA and SF are provided by the supplier and are presented in Table 1. Since RHA and SF possess very high SiO_2 content (>90 %, refer to Table 1), they are both regarded as highly pozzolanic materials.

Table 1
Chemical compositions of RHA and SF.

Chemical composition (%)	RHA	SF
Magnesium oxide (MgO)	0.77	0.41
Aluminium oxide (Al_2O_3)	0.46	0.50
Iron oxide (Fe_2O_3)	0.43	0.06
Silicon dioxide (SiO_2)	90.00	94.58
Calcium oxide (CaO)	1.10	1.54
Potassium oxide (K_2O)	4.60	0.64
Sodium oxide (Na_2O)	—	0.23
Phosphorous pentoxide (P_2O_5)	2.43	0.11
Sulphate (SO_3)	—	0.14
Loss of ignition	3.90	1.79

In this study, silica sand (SS) and ceramic powder (CP) serve as fine aggregates in the concrete mixes, instead of quartz powder and quartz sand. The specific gravity and bulk density of SS were 2.0 – 2.7 and 2200 kg/m^3, respectively. While SS had a median particle size of 300 μm, CP obtained by pulverising ceramic sanitary ware (see Fig. 2) was 15 μm in size. With this small particle size, CP was expected to partially serve as a SCM. The chemical compositions of SS and CP are tabulated in Table 2.

Sika® ViscoCrete® PC HRF-1 superplasticizer (SP) having a density of 1.09 g/cm^3 and a pH of 6 was utilised to reduce the water content and improve the workability of the concrete mixes. Since 13-mm-long fibres, which was considered as long fibres, are more efficient in preventing the development of macro-cracks within the UHPC matrix [36], brass-coated 13-mm long steel fibres (see Fig. 3) were added to increase the flexural strength and durability of the UHPCs in this study. The chemical, physical and mechanical features of steel fibres are tabulated in Table 3.

2.3. Design mixture proportioning

Four batches and a total of twelve mixtures were designed to investigate the influence of RHA and CP replacement on the workability and mechanical characteristics of UHPC. While the steel fibres proportions in UHPCs studied in the literature was usually chosen to be 1.5–2 % [13,37], mixtures with two different amounts of steel fibres were designed to examine possible effects of steel fibres on mechanical and damping properties of UHPCs. In this study, the steel fibre amounts in batches B2, B3, and B4 remained at 2 % of the total volume, whereas batch B1 contained 1.2 %. Furthermore, SF was substituted with 5 %, 10 %, and 15 % RHA in batches B1 and B2, batch B3 replaced cement with RHA at percentages of 10 %, 15 %, and 20 %. These replacing proportions were investigated based on previous research works [9, 27–33] in which RHA was found to enhance mechanical properties of concrete mixes. The mixture that demonstrated the highest compressive strength in all examined mixtures of batches B1 and B2, served as the base design for batch B4 in the second stage of the experimental programme.

In stage Two, the amount of SS was partially substituted with CP at

Fig. 1. Physical appearance of RHA.

Fig. 2. Physical appearance of CP.

Table 2
Chemical compositions of SS and CP.

Chemical Composition (%)	SS	CP
Magnesium oxide (MgO)	0.1	1.8
Aluminium oxide (Al_2O_3)	22.2	0.7
Silicon dioxide (SiO_2)	65.8	92.5
Calcium oxide (CaO)	0.1	0.5
Potassium oxide (K_2O	3.5	0.8
Sodium oxide (Na_2O)	1.0	0.5
Titanium Dioxide (TiO_2)	0.3	0.3
Other	7.0	2.9

Fig. 3. Copper coated steel fibres.

Table 3
Mechanical properties of steel fibres.

Mechanical properties	
Diameter	0.2 mm
Aspect ratio (*L/D*)	65
Density	7,800kg/m^3
Tensile strength	> 2300MPa
Young's modulus	200GPa
Elongation (%)	0.5 – 4.0

10 %, 15 %, and 20 %. The common mix, consisting of cement, SF, FA, SS, and steel fibres, was used as the reference. For all mixtures, the water-to-binder (w/b) ratio along with the quantities of FA and SP were kept constants at 0.175, 77.1 kg/m^3, and 67 kg/m^3, respectively. These figures were selected based on an investigation on the behaviour of RHA-based UHPC [38]. Details of mix designs are provided in Tables 4 and 5. Note that the mixtures' labels represent the partially replaced materials, their substitutions along with the replacing proportions, and the steel fibre percentage. For example, the RSF5–1.2 mixture replaced

Table 5
Mixture designs in Stage 2 (kg/m^3).

Material	Stage 2 (SF replaced with RHA & SS replaced with CP)		
	B4		
	RS5-CP10-2	RS5-CP15-2	RS5-CP20-2
Cement	800	800	800
SF	146.3	146.3	146.3
FA	77.1	77.1	77.1
RHA	7.7	7.7	7.7
SS	934.74	882.81	830.88
CP	103.86	155.79	207.72
Water	180	180	180
SP	67	67	67
Steel fibre	156	156	156
Water-to-binder ratio	0.175	0.175	0.175

SF with 5 % of RHA and employed 1.2 % of steel fibres, whereas mix RCF10–2 substituted cement with 10 % of RHA and employed 2 % of steel fibres. In these mixtures' labels, "S" means silica fume and "C" indicates cement.

2.4. Specimen preparation and test methods

Concrete mixing and testing were conducted at the concrete lab, conforming with AS 1012.2:2014 [39] and AS 1012.8.1:2014 [40]. At the beginning, all the dry materials (cement, SF, FA, RHA, SS/CP) were dry mixed in a 10 Litre Planetary Mixer for five minutes at medium speed, to obtain a homogeneous mixture and prevent particle agglomeration. Next, a mixture of 80 % of the required amount of water and 100 % of SP was gradually added to the dry mix; and mixing continued for five minutes at a higher speed. Then, the remaining water was gradually poured into the liquidised mixture and mixed for another six to seven minutes. Finally, when the mixture had grown moist and gained appropriate consistency, steel fibres were slowly added and mixed for another six minutes to be evenly dispersed in the mixture. This must be done as clumped or clustered fibres may induce to localised stress concentration that may potentially lead to premature failure of UHPC specimens.

Workability of the freshly mixed UHPC was determined by a slump flow test, which is conducted in accordance with AS 1012.3.5:2015 [41]. When ready, the prepared mixture was placed into a mini slump cone (illustrated in Fig. 4) that had a height of 50 mm and top and bottom diameter of 70 mm and 100 mm, respectively. The cone was then lifted up slowly, allowing concrete mix to flow out and spread. After two minutes, the diameter of the spread mix, called the slump flow diameter, was measured as shown in Fig. 5. According to ASTM C143, the acceptable average slump diameter of two perpendicular directions should be between 175 mm and 300 mm.

Once the slump flow test was finished, the mixture was poured into the moulds in 1/3 layers of height with 30 s of vibration for each layer. Then specimens were kept in the moulds for 24 hrs at atmospheric

Table 4
Mixture designs in Stage 1 (kg/m^3).

Material	REF	Stage 1 (cement or SF replaced with RHA)							
		B1		B2			B3		
		RS5-1.2	RS10-1.2	RS5-2	RS10-2	RS15-2	RC10-2	RC15-2	RC20-2
Cement	800	800	800	800	800	800	720	680	640
SF	154	146.3	138.6	146.3	138.6	130.9	154	154	154
FA	77.1	77.1	77.1	77.1	77.1	77.1	77.1	77.1	77.1
RHA	0	7.7	15.4	7.7	15.4	23.1	80	120	160
SS	1039	1039	1039	1039	1039	1039	1039	1039	1039
Water	180	180	180	180	180	180	180	180	180
SP	67	67	67	67	67	67	67	67	67
Steel fibre	156	100	100	156	156	156	156	156	156
Water-to-binder ratio	0.175	0.175	0.175	0.175	0.175	0.175	0.175	0.175	0.175

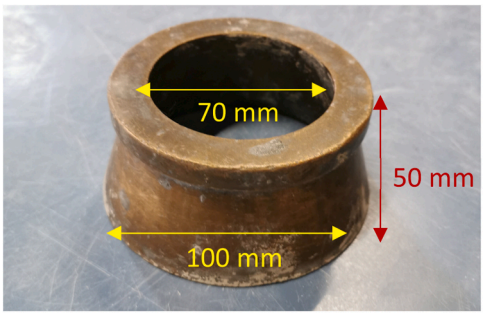

Fig. 4. Mini cone for slump test.

Fig. 5. Slump flow diameter of reference mix.

temperature (20 °C) and 95 % relative humidity (RH). While 50×50×50 mm cubes were cast for the compression test, and 40×40×160 mm beams were cast for flexural and damping test. These specimen sizes were selected as they are frequently adopted in compressive and flexural tests for ultra-high performance steel fibred concrete [5,8,36,42,43]. After demoulding, all samples were steam cured for 72 h at a temperature of 85 °C.

The compressive test was performed following ASTM C109/C109M-13 [44] and using MATest UTM 2000 kN test machine. To ensure reliable outcomes, six identical samples were tested for each mixture.

The damping test was conducted on all mixtures; each had triplicate samples. While the ASTM E756–05 provides the Oberst Beam Method (OBM) to determine the damping properties of materials [45], this method is not recommended for concrete. Based on the concept of OBM, the authors introduced a modified experimental procedure and setup, as illustrated in Fig. 6(a). Specifically, a clamp apparatus was to fix one end of a beam specimen. While a rubber-headed hammer gently struck the tested beam, free oscillations of the beam at the free end, mid-span, and fixed end were collected through accelerometers. Digital signals were transferred to an HBM data logger (see Fig. 6(b)) and converted to frequency domain (FFT) using MATLAB computer programme (see Fig. 7). During the experiment, the sampling rate was set to 1200 Hz.

The damping ratio (ξ) was then determined by analysing the wave

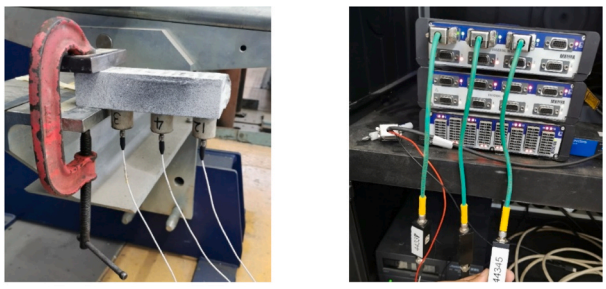

(a) **(b) HBM data logger for accelerometers**

Fig. 6. (a). Damping test setup, (b) HBM data logger for accelerometers.

using the logarithmic decrement method as explained in Eq. (1), and expressed as:

$$\xi = \ln\left(\frac{Y_1}{Y_2}\right) \times \frac{1}{N(2\pi)} \times 100 \quad (\%) \tag{1}$$

where: Y_1 is the maximum magnitude of the wave; $Y_2 \approx 0.5Y_1$; and N is the number of cycles between Y_1 and Y_2.

Flexural behaviours of the newly designed UHPC were determined as per ASTM C78/C78M-22 [46]. Accordingly, four-point flexural tests were conducted on 40×40×160 mm beam specimens, using a SHIMADZU 300 universal test machine. A laser sensor was used to measure the mid-span deflection. The loading rate of 0.8 kN/min was calculated using Eq. (2) given in the ASTM standard. Considering the restrained timeframe and availability of the UTM, the loading rate was increased to 1.6 kN/min. Fig. 8 describes the flexural test set up. The loading rate (r) is determined using Eq. (2):

$$r = \frac{Sbd^2}{L} \tag{2}$$

where S is the rate of increase in maximum stress on the tensile face in (kPa/min); L is the span length (m); and b and d are respectively the average width and depth of the specimen (m).

3. Results and discussions

3.1. Workability

Fig. 9 presents the slump flow values of all tested mixtures. Overall, all mix designs experienced a reduction of workability in comparison with the control mix. Compared to the REF mix, the workability of the B1′s mixtures reduced by 10.9 % and 14.9 %, respectively for 5 % and 10 % RHA substitutions. A negative tendency was also observed for mixes in batch B2, indicating the negative impact of RHA replacement on the fresh UHPC. While RHA has a larger particle size than SF (as indicated in Section 2.1), its specific surface area was actually higher due to its porous structure [3,14,16,47]. An increase in RHA content resulted in a higher total surface area of the binder, leading to greater water absorption and consequently reducing the rheology of mixtures [3,16,17,47]. Additionally, SF could provide lubrication to a fresh concrete mix due to its spherical particle shape [3]. Increasing the amount of SF substitution with irregularly shaped RHA particles reduced this lubricant effect of SF, resulting in a gradual fall in the slump flow diameters regarding the same amount of water. This observation was also reported in [10]. Therefore, the experimental results in this study, supported by other research, suggested that replacing SF with RHA marginally compromise the workability of concrete mixes.

While substituting SF with RHA slightly affected the UHPC's rheology, partially replacing cement with RHA demonstrated very poor workability. From Fig. 9, the slump flow diameters of B3′s samples decreased significantly by 45.5 %, 53.8 %, and 63.7 %, respectively with 10 %, 15 %, and 20 % RHA replacement compared to the control mix. Similar to SF, this could be attributed to the much greater surface area of RHA in comparison with that of cement, which led to absorption of more water [48]. Another reason may be ascribed to an increase in volume of the mixture when adding RHA and keeping the density and total weight of binders constant (see Table 4). As stated in previous studies [49,50], this volume increase resulted in decreased rheology of the mix due to an increase in the plasticity and cohesiveness.

While substituting SF with RHA slightly affected the UHPC's rheology, partially replacing cement with RHA demonstrated very poor workability. From Fig. 9, the slump flow diameters of B3′s samples decreased significantly by 45.5 %, 53.8 %, and 63.7 %, respectively with 10 %, 15 %, and 20 % RHA replacement compared to the control mix. Similar to SF, this could be attributed to the much greater surface area of RHA in comparison with that of cement, which led to absorption

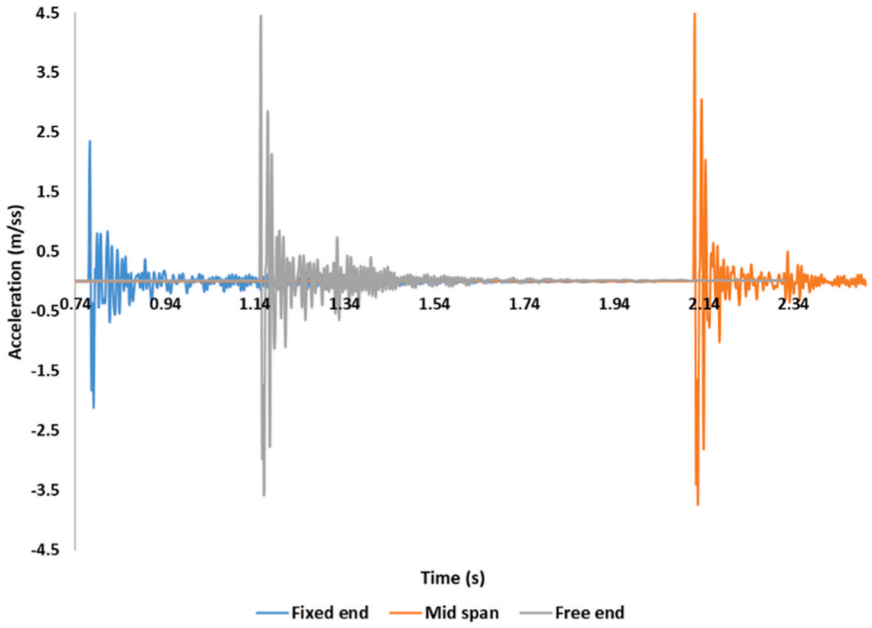

Fig. 7. The logarithmic decrement signals of RS5–2.

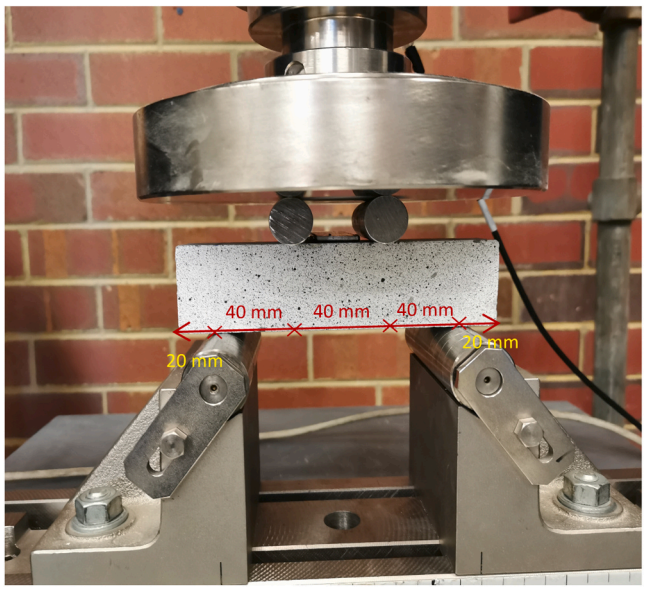

Fig. 8. Flexural test setup.

of more water [48]. Another reason may be ascribed to an increase in volume of the mixture when adding RHA and keeping the density and total weight of binders constant (see Table 4). As stated in previous studies [49,50], this volume increase resulted in decreased rheology of the mix due to an increase in the plasticity and cohesiveness.

Regarding batch B4, a reduction in rheology was observed with an increase in percentages of CP replacement while keeping a constant quantity of RHA (5 %). The slump flow diameters of this batch's mixtures dropped by 6.6 %, 10.9 %, and 25.7 %, respectively for 10 %, 15 %, and 20 % of CP replacement. Again this pattern could be explained by the high water absorption in the concrete pastes in the presence of fine ceramic particles having large surface area than SS [51].

In general, due to high values of surface area of both RHA and CP, the workability of the newly designed UHPCs in this study was reduced, and this issue can be mitigated by using SP or FA.

3.2. Compressive capacity

Fig. 10 presents the compressive strengths of all the mixtures. For both batches B1 and B2, replacing SF with RHA resulted in a considerable growth in the compressive strength, with increments of 6.6–25.6 % compared with the REF mix (132.6 MPa). Specifically, the RS5–2 mixture possessed the largest compressive strength, at 166.5 MPa, followed by RS10–2 and RS15–2, at 163.9 MPa and 147.1 MPa, respectively. These promising outcomes well agreed with those reported in [17], which could be attributed to the improved pozzolanic reactivity, and filling and internal curing effects of RHA [25]. Moreover, adding more steel fibres to the mixtures induced to a rise in the compressive strength. When increasing the steel fibre content from 1.2 % to 2 %, the compressive strengths of RS5–2 and RS10–2 rose by 15.1 % and 10.1 %, respectively compared to RS5–1.2 and RS10–1.2 counterparts. This upward pattern was also documented in previous studies [36,47,52]. According to these researchers, the addition of fibres to the cementitious mixtures creates a strong network in the matrix, bridges cracks, and increases the strength considerably, but further increase in the fibre content will negatively affect workability [36,47].

For different quantities of steel fibres, increasing the replacement percentage of RHA led to opposite patterns. As the RHA ratio increased from 5 % to 10 %, Batch B1 exhibited a 4.2 % rise in compressive resistance. In contrast, the compressive strengths of B2′s mixtures declined by 1.6 % and up to 11.6 % with 10 % and 15 % RHA dosage, respectively. There was an interaction between the quantity of steel fibres and the substitution amount of RHA for SF. More experimental works should be carried out to determine the optimum mix design considering both steel fibres and RHA.

Regarding batch B3, it is apparent that partially replacing cement with RHA had a considerable impact on the UHPC's compressive capacity. Except for RC20–2, the compressive strengths of RC10–2 and RC15–2 were 11.6 % and 14.9 % respectively higher than the control specimens. These advantageous results were supported by findings of previous studies [24,53,54], which could be ascribed to the micro-filling ability and pozzolanic characteristics of RHA. Not only can RHA fill in the microscopic gaps within the cement particles, it reacts with water and calcium hydroxide to produce additional C-S-H (calcium silicate hydrates) gel [24]. This additional C-S-H reduces the porosity of concrete by filling the capillary pores, and therefore enhances the

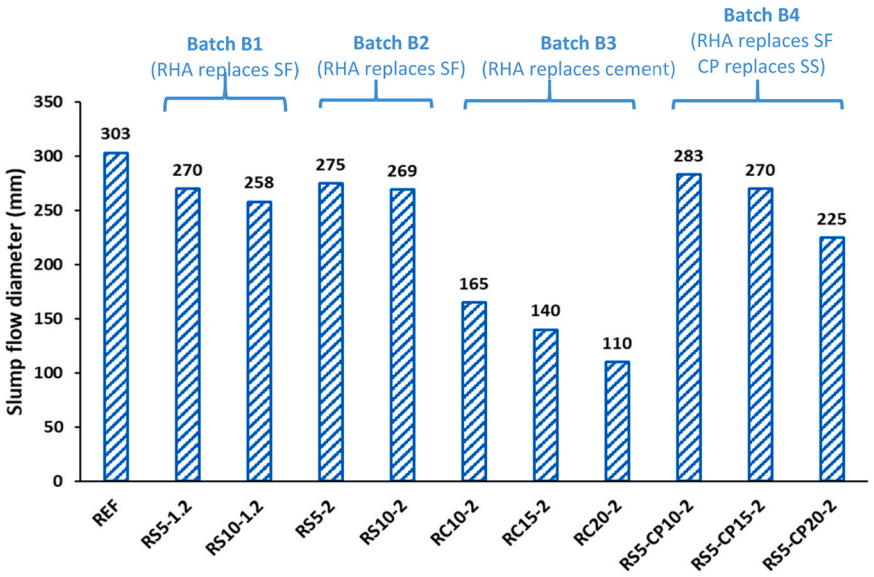

Fig. 9. Slump flow diameters of all mixtures.

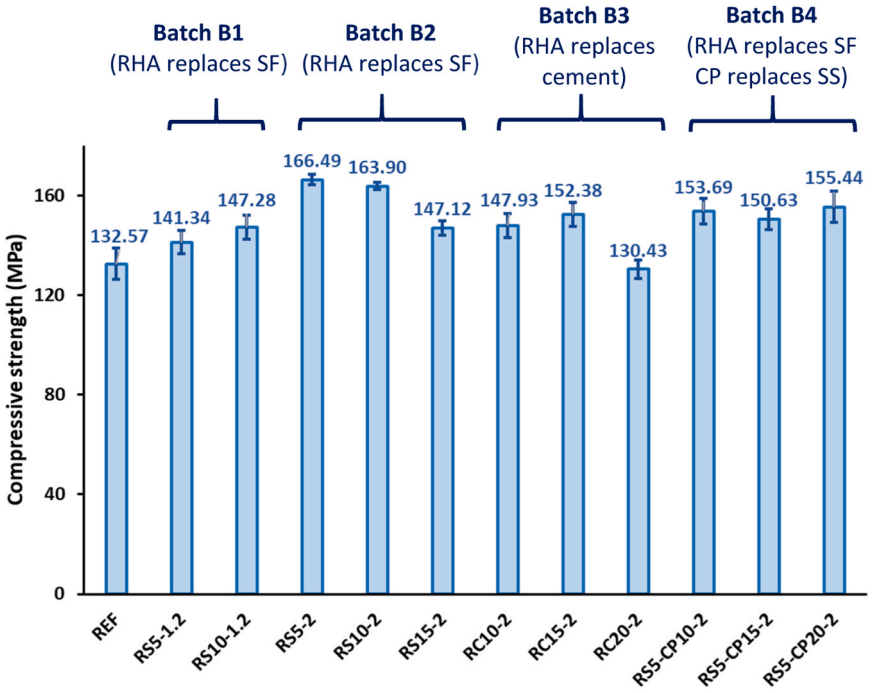

Fig. 10. Compressive strengths of all mixtures.

microstructure of the concrete paste.

Regarding batch B3, it is apparent that partially replacing cement with RHA had a considerable impact on the UHPC's compressive capacity. Except for RC20–2, the compressive strengths of RC10–2 and RC15–2 were 11.6 % and 14.9 % respectively higher than the control specimens. These advantageous results were supported by findings of previous studies [24,53,54], which could be ascribed to the micro-filling ability and pozzolanic characteristics of RHA. Not only can RHA fill in the microscopic gaps within the cement particles, it reacts with water and calcium hydroxide to produce additional C-S-H (calcium silicate hydrates) gel [24]. This additional C-S-H reduces the porosity of concrete by filling the capillary pores, and therefore enhances the microstructure of the concrete paste.

On the other hand, when substituting 20 % amount of cement with RHA, the compressive capacity of the RC20–2 specimens dropped trivially (less than 2 %). The average compressive strength of RC20–2 was 130.4 MPa, which was comparable to the control mix (132.6 MPa). Apparently, with over 20 % replacement percentage, the merit of RHA incorporation was negated. This observation aligns with a previous study [55]. However, Gastaldini et al. [21] and Chindaprasirt et al. [20] collectively affirmed that a cement substitution of up to 20 % RHA could still elevate the compressive resistance of the concrete blends. According to He et al. [56], the influence of RHA on concrete compressive capacity depend on many factors, including the replacement level, water-to-binder ratio and genre of binders. Additionally, the mixtures in this study were steam cured, whereas previous research utilised wet curing regime [20,21]. More experimental works, especially on UHPC, should be conducted to clarify the true impact of replacing cement with

RHA at higher levels on concrete compressive resistance.

In the presence of both RHA and CP, B4′s mix attained a 13.6–17.2 % rise in the compressive strength compared to the control samples (see Fig. 10). Siddesha [57], on the other hand, observed decreased compressive strength in concrete mixtures having 10–20 % fine ceramic aggregates. Considering an addition of 5 % RHA, concrete samples containing up to 20 % CP replacement still exhibited enhanced compressive strength, indicating the advantageous synergic effect of RHA and CP addition. The performance of B4′s mixtures with up to 20 % CP demonstrated minor variation (<2 %) regarding those of 5 %CP, indicating no definitive conclusion about the impact of increasing CP substitution level on the UHPC's compressive capacity.

In general, the experimental results suggested that replacing SF by RHA yields higher compressive strength than substituting cement by RHA and the optimal mix design for the highest compressive strength was to replace 5–10 % CF by RHA and use 2 % steel fibre. Simultaneously incorporating RHA (5 %) and CP (up to 20 %) yielded synergistic effects and thus good performance of UHPC.

3.3. Flexural capacity and load deflection curves

Fig. 11 presents the flexural strengths of all twelve mixtures. Accordingly, no explicit trend was observed for the impacts of different steel fibre contents on the bending capacity of UHPC blends when comparing batch 1 and batch 2. Considering SF substitution, enhanced flexural strengths were achieved with an increase in RHA replacement proportions, up to 15 %. Specifically, the flexural strength of RS10–1.2 was 4.1 % and 10.3 % higher than that of the REF and RS5–1.2 samples, respectively. Similarly, RS5–2 and RS15–2 mixtures attained a 4.0 % and 31.2 % rise in the bending strength compared to the control mix, respectively. Regardless of fibre content, up to 10 % RHA replacement exhibited a comparable flexural strength, whereas mixture having 15 % RHA dosage with 2 % steel fibre demonstrated a significant increase in the bending capacity. This positive influence of RHA substitution for SF was in line with those reported in [13,58].

Compared to the REF specimens, B3′s mixtures showed greatly enhanced flexural resistance, with increments of 41.2 %, 43.5 %, and 46.1 %, respectively for 5 %, 10 %, and 15 % RHA. These findings aligned with existing studies [12,37,53,59,60]. For instance, Alyami et al. [37] found the RHA-incorporated UHPCs exhibited 5.6 %, 11.5 %, and 5.1 % higher flexural strengths than that of RHA-free counterpart, respectively for 10 %, 20 %, and 30 % RHA. Bie et al. [53], when investigating the effects of different burning conditions of RHA on concrete pastes, discovered that 20 % RHA, heated at 700 °C, led to an approximately 58 % increment in flexural capacity of RHA-based concrete. In a study of reactive powder concrete containing synthesised RHA, Alkhaly et al. [12] observed that the addition of up to 30 % RHA intensified the flexural strength, regardless of curing regimes. Similar to what was observed for compressive capacity, this rise in bending resistance resulted from the pozzolanic reactions and pore-filling effect occurring within the concrete mixture [24,61,62].

The combined effect of substitution of both RHA and CP in batch B4 displayed significant improvements in the flexural capacity, which were 47.9–59.1 % higher than that of the control mix. From Fig. 11, RS5-CP15–2 and RS5-CP20–2 specimens exhibited the highest bending strength, at about 37 MPa. When increasing the CP ratio from 10 % to 15 %, the bending capacity of CP-incorporated mixtures grew by 7.6 %. However, when the CP substitution quantity reached 20 %, a comparable bending performance was observed for both RS5-CP15–2 and RS5-CP20–2 UHPC mixes. These outcomes are different from those presented in [30,57,63], in which these studies found a decline in the flexural capacity as the replacement ratio of CP increased. While Siddesha [57] observed a marginal decrease in flexural resistance of concrete with the increasing dosage of CP, Canbaz [30] reported a substantial loss (70 %) of flexural strength in concrete having 25–100 % CA compared to natural aggregate concrete. Meanwhile, the designed mixtures in this study contained RHA and CP simultaneously. The great advantages of RHA may have compensated for the negative effects of CP, resulting in an overall improved flexural performance.

The relationship between mid-span deflection and flexural load of beam specimens is depicted in Fig. 12. It is noted that the data for RS5-SF2 was excluded due to a malfunction. From Fig. 12 (a), different RHA replacement levels for SF showed a minor impact on the behaviour of the load-deflection curves. Compared to the reference mix, the first two batches exhibited similar slopes in the ascending portion of load-displacement curves. This suggested that the presence of RHA did not significantly change the flexural stiffness of the UHPCs mixtures, regardless of different ratios of steel fibres. Except for RS10–2, other

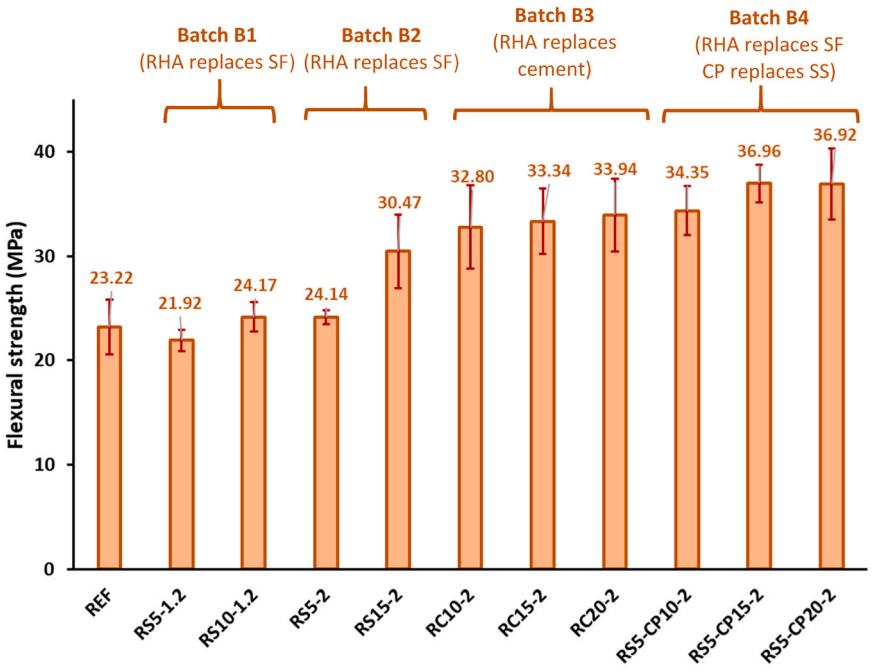

Fig. 11. Flexural strengths of all mixtures.

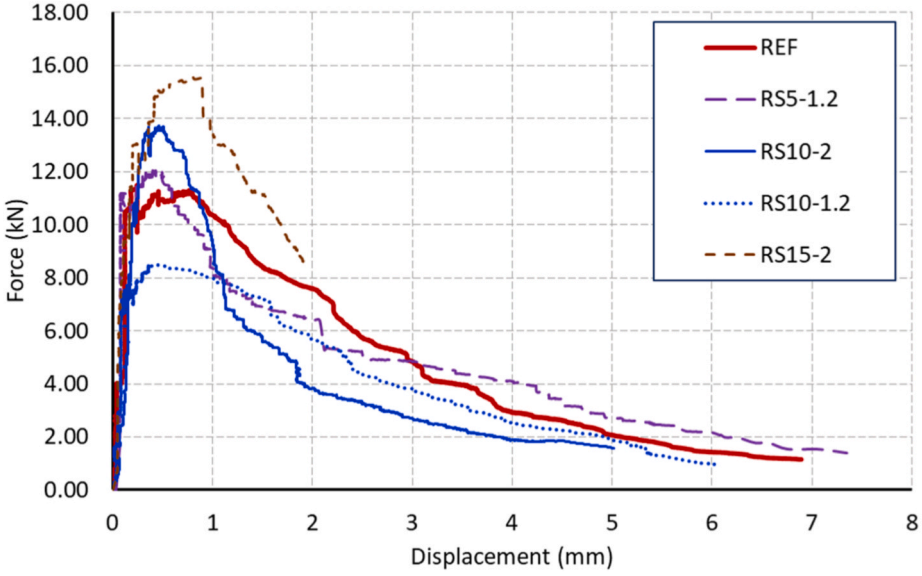

(a). REF and batches B1, B2

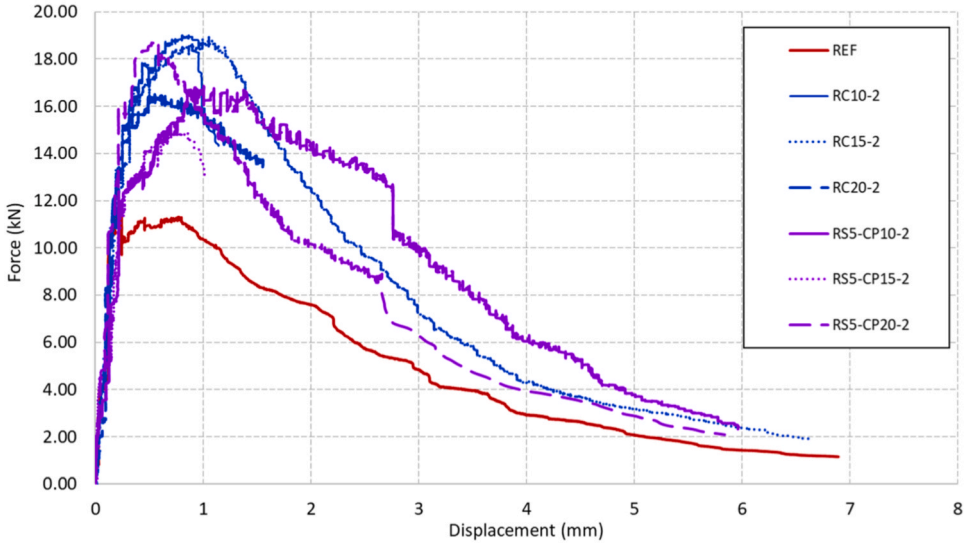

(b). REF and batches B3, B4

Fig. 12. Load-deflection: (a) REF and batches B1, B2 and (b) REF and batches B3, B4.

mixes showed 4.3–39.1 % higher peak loads than that of the control mix. Considering the same dosage of steel fibres, increasing the RHA replacement level induced to higher peak loads, from 12 to 13.5 kN for B1 and 8.4 to 15.5 kN for B2. Noticeably, RS10–1.2 and RS15–2 specimens experienced a sudden drop in the load-deflection graph, indicating more brittle behaviour in comparison with their other counterparts. While the RS15–2 mixture showed a drastic rupture at 2 mm of deflection, others fractured completely at beyond 5 mm, exhibiting higher ductility that is desirable for energy absorption under seismic loads.

As can be seen from Fig. 12 (b), the control mix, batches B3, and B4 had comparable slopes in the ascending part of the load-deflection curves. This suggested that different replacement dosages of RHA for cement and of CP for SS had minor impacts on the flexural stiffness and rigidity of the UHPC mixes. Notably, B3's mixtures demonstrated 40–65 % higher ultimate flexural forces compared to the control mix. This great enhancement could be ascribed to the presence of RHA in the concrete mix, which improved the crack-bridging capacity of fibres against the pulling action of the imposed load [59]. Interestingly, while other samples experienced sudden ruptures upon reaching peak loads, the RC20–2 showed steady displacement without further increases in flexural load, indicating that the inclusion of RHA and CP in UHPCs could have elongated the strain hardening phase during samples bending failure.

3.4. Damping ratio

The damping ratio evaluates the ability to dissipate energy of a concrete structure, which is essential to ensure the resilience of a structure in incidence of critical hazards (e.g., earthquake). In prior investigations, the damping ratio of uncracked concrete fell within the range of 0.32 % to 0.64 %, whereas in the presence of cracks, the values extended from 1.3 % to 2.1 % [64]. Additionally, other studies have collectively reported that the damping ratio of standard concrete was below 5 % [65–67]. Fig. 13 presents the damping ratios of all tested

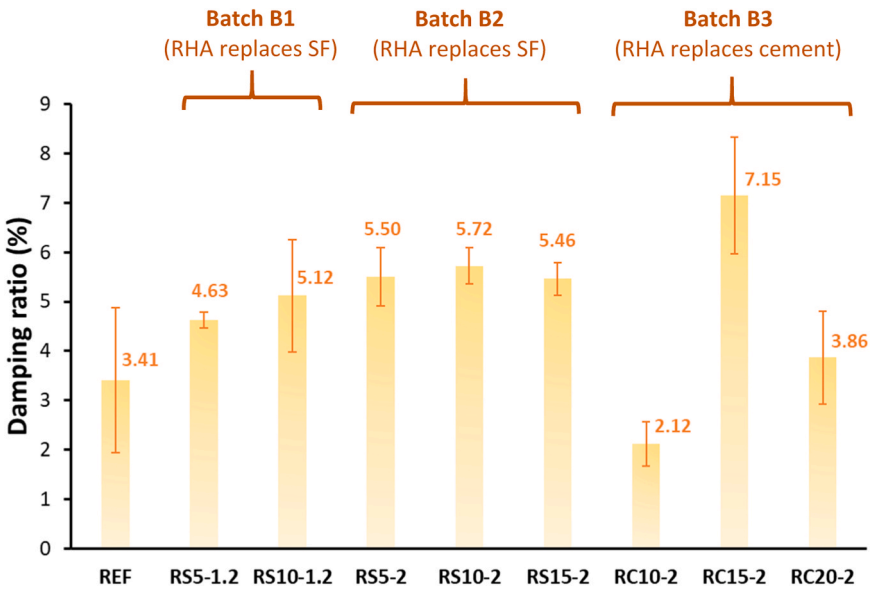

Fig. 13. Damping ratios of mixtures.

mixes in this study.

The damping ratio of the control UHPC mixture was 3.41 %, which was consistent with findings in a previous study by Xi et al. [68]. Depending on different testing methods, UHPC containing 10 % SF, 10 % FA, and 20 % slag had a damping ratio of 2.36–3.73 %. Apart from RC10–2, the damping ratios of designed mixes were 1.13–1.95 times higher than that of the control samples. This indicated that the UHPC mixtures could dissipate energy faster with the addition of RHA. For both batches B1 and B2, increasing the RHA replacement proportion from 5 % to 10 % induced to considerably enhanced damping property. Compared to the control mix, RS5–1.2 and RS10–1.2 specifically possessed a 35.7 % and 50 % improvement, respectively. Similar positive trend was obtained for batch B2, with even greater increments of 61.2 % and 67.7 %, respectively for 5 % and 10 % RHA.

However, when the percentage of RHA rose to 15 %, the damping ratio of RS15–2 was equal to that of RS5–2, which was 4.6 % smaller than the RS10–2′s one. This suggested that substituting more than 15 % of SF with RHA could decrease the extent of improvement in UHPC's damping performance. This indicated that there was an optimal balance between the pozzolanic activity of RHA and its bonding characteristics within the UHPC matrix. Beyond a certain threshold, the additional RHA no longer effectively contributed to enhancing the ITZ, potentially leading to a levelling off or even a decline in damping efficiency. Besides, as the proportions of steel fibres increased in the concrete paste, both RS5–2 and RS10–2 achieved 11.8–18.8 % higher damping ratios than those of their counterparts having 1.2 % of steel fibres by volume. As expected, the incorporation of steel fibres augmented the crack-bridging ability and energy absorption capacity of the UHPC [36,47], thereby improving its damping performance. From the obtained results, it is evident that RHA and steel fibres together improved the damping ratios of UHPC mixtures. While the fibres enhanced energy dissipation within mixes through friction and pull-out resistance, the added RHA refined the microstructural density and bonding characteristics.

Except for RC10–2, B3′s mixtures exhibited greater damping performance than the control mix. While the damping ratios of specimens in batch B3 were less consistent than those of batches B1 and B2 and the associated reason was not clear, the enhancement levels in damping ratio were far lower than those of the first two batches. Replacing cement with RHA was not as effective in enhancing damping performance as substituting SF, similar to the results observed for compressive capacity. Still, the damping ratios of B3′s mixes increased with the rise in the RHA replacement ratio, suggesting a positive correlation between the amount of RHA and the withstandability of UHPC in case of extreme loadings. Overall, while there are inconsistencies requiring further research, these outcomes suggested that appropriately increasing the quantity of steel fibres and the substitution proportion of RHA could enhance the energy dissipation capability of the UHPC mixtures. The increase in damping ratios aligns well with improvements in the flexural strength. This emphasised the potential of RHA as a supplementary material to improve the damping performance of UHPCs, particularly when combined with an appropriate level of steel fibres. By optimising the contents of RHA and steel fibres, the damping properties of UHPC can be tailored to meet specific performance requirements, thereby broadening its applicability in various engineering contexts.

4. Environmental impact assessment

As mentioned earlier, one of the primary objectives of incorporating RHA and CP in the concrete mix is to mitigate the adverse environmental impacts of concrete production. To appraise the sustainable performance of the tested UHPCs, the total equivalent embodied carbon (EC_{total}) of each mix was estimated and compared with the control mix. Since steam curing requires heating energy, its associated emissions were also considered. As quantified by Turner and Collins [69], the carbon footprint of steam curing is 2.49 $kgCO_2/m^3/h$. In this research, tested specimens underwent a three-day curing process (72 h), including a gradual heating period of four hours. Hence, the CO_2 emissions of the steam curing process were determined as: $76h \times 2.49 kgCO_2/m^3/h = 189.24 kgCO_2/m^3$.

The EC_{total} of a UHPC blend was quantified by aggregating CO_2 emissions released from the production of its constituent materials and the steam curing process. Notably, this study considered the embodied impacts of UHPC mixtures within the "cradle-to-gate" boundary system, meaning the transportation of raw materials and their availability were excluded in the assessment. Due to considerable variations in the availability of raw materials across different locations, this factor was not considered in this simple and initial evaluation. Besides, the environmental impacts of the production stage are generally more significant than the transportation stage, results of comparison are expected to fluctuate marginally, maintaining the overall tendency [70]. Therefore, the current approach offers an acceptably accurate initial evaluation, showing the primary contributors to the sustainability of the designed UHPCs. Specifically, the component EC was calculated by multiplying the *EC* intensity (provided in Table 6) of each material (EC_i) by its

Table 6
The *EC* of the raw materials.

Raw materials	*EC* ($kgCO_2/kg$)	Reference
Cement	0.8300	[71]
SF	0.0140	[72]
FA	0.0270	[69]
RHA	0.1032	[71]
SS	0.0100	[71]
CP	0.0450	[73]
Water	0.0003	[71]
Steel fibre	1.4965	[71]
SP	0.7200	[71]

corresponding mass (m_i), as shown in Eq. (3).

$$EC_{total} = \sum EC_i m_i \tag{3}$$

Table 7 presents the EC_{total} of all twelve mixtures. Due to the decreased quantity of steel fibres, the total EC of B1′s mixtures were about 7.2 % lower than that of the conventional mix (1149.6 $kgCO_2$). Given the significantly high EC intensity of steel compared to other materials (refer to Table 6), even a slight decrease of 0.8 % in steel fibres led to an apparent change in the mixture's CO_2 emissions. On the other hand, the embodied impacts of B2′s samples were roughly equal to that of the REF mix, despite having 5–15 % RHA ratio. This could be ascribed to the much larger carbon intensity of RHA compared to SF (see Table 6), which led to a final rise in total EC of B2′s UHPCs. Considering batch B3 (replacing cement with RHA), raising the RHA content from 10 % to 20 % increased carbon savings, by 5.1–10.1 % compared with the control mix (see Table 7). Notably, substituting RHA for cement was more environmentally friendly than for SF, which was due to the fact that RHA had a larger EC coefficient than SF but was less carbon intensive than cement (see Table 6). Regarding the last batch, the EC figures were marginally higher than that of the control counterpart. Despite variations in CP replacement content (10–20 %), B4′s mixtures showed minor differences in their final carbon footprints. Broadly speaking, all developed mixtures yielded either superior or comparable sustainable performance to the conventional UHPC.

To determine the optimal UHPC that has superior compressive/flexural strength and sustainable performance, a normalised compressive carbon index (CI_c) (see Eq. (3)) and flexural carbon index (CI_f) (see Eq. (4)) were analysed.

$$CI_c = \frac{EC_{total}\left(\frac{kgCO_2}{m^3}\right)}{Compressive\ strength(MPa)} \tag{3′}$$

$$CI_f = \frac{EC_{total}\left(\frac{kgCO_2}{m^3}\right)}{Flexural\ strength(MPa)} \tag{4}$$

Fig. 14 describes the compressive and flexural carbon indexes of designed mixes. Overall, tested mixtures were less carbon intensive than the control mix, indicating the advanced eco-efficiency of the proposed mix designs. Compared to the conventional mix, the CI_c values of the first batch were 13–16 % smaller, which was owing to their higher compressive strengths (refer to Fig. 10) and lower carbon footprints (refer to Table 7). Although CI_c figure of RS15–2 remained lower than the REF's, it became evident that the carbon efficiency of B2′s mixtures reduced when the RHA substitution ratio reached 20 %. For batch B3, increasing the cement substitution ratio from 10 % to 15 % decreased the carbon index by 14.9–19.6 %, the value began to rise at a 20 % replacement. Meanwhile, the last batch, having comparable compressive resistance and sustainable performance, showed minor changes in carbon indexes with different CP replacement proportions.

Similar to the compressive carbon index, the CI_f values of studied mixtures were generally smaller than the control mix. Apart from RS10–2, raising the RHA content reduced the flexural carbon indexes of the first two batches, by 1.7–23.6 % compared with the REF mix. Considering batch B3, it was explicit that increasing the RHA substitution ratio induced to lower bending carbon indexes. The CI_f figures for B3′s mixtures dropped significantly, by 32.8–38.5 %. Batch B4, incorporating both RHA and CP, also obtained a substantial reduction in CI_f indexes, ranging from 32.1 % to 36.8 %. Given the consistently enhanced carbon efficiency with up to 20 % CP replacement, future research should explore higher replacement ratios of CP to determine the ultimate optimum percentage.

As shown in Fig. 14, RS5–2 was the best mixture considering compressive strength, whereas RC20–2 demonstrated the smallest flexural carbon index. However, when mechanical and environmental performance were together considered, RC15–2 appeared to be the superior mixture, exhibiting < 1 % higher CI_c and 4.7 % higher CI_f than RS5–2 and RC20–2, respectively. This balance made RC15–2 the most effective choice for achieving excellent performance in both strength metrics and sustainability.

5. Cost analysis

In this section, the economic efficiency of the RHA-based UHPC mixtures were assessed. Table 8 provides the unit prices of the component materials in Australian dollar (AUD). Note that the production costs of RHA and CP were converted from USD to AUD, using the corresponding exchange rate of the reported year [74,75]. The production costs of mixtures were calculated as a sum of constituent materials' costs. It is worth emphasising that these considered costs may not represent the actual production costs because the materials' prices can fluctuate depending on the supplier and product availability. As the availability of raw materials greatly varies across countries and regions, this factor was omitted for the purpose of simple estimation and initial evaluation. In this analysis, material costs were estimated based on the

Table 7
Total *EC* of the studied mixtures.

		Compositions										EC_{total} ($kgCO_2/m^3$)
		Cement	SF	Fly ash	RHA	SS	CP	Water	SP	Steel fibre	Curing	
REF		664.00	2.16	2.08	0.00	10.39	-	0.05	48.24	233.45	189.24	1149.61
B1	RS5 −1.2	664.00	2.05	2.08	0.79	10.39	-	0.05	48.24	149.65	189.24	1066.49
	RS10 −1.2	664.00	1.94	2.08	1.59	10.39	-	0.05	48.24	149.65	189.24	1067.18
B2	RS5 −2	664.00	2.05	2.08	0.79	10.39	-	0.05	48.24	233.45	189.24	1150.30
	RS10 −2	664.00	1.94	2.08	1.59	10.39	-	0.05	48.24	233.45	189.24	1150.99
	RS15 −2	664.00	1.83	2.08	2.38	10.39	-	0.05	48.24	233.45	189.24	1151.67
B3	RC10 −2	597.60	2.16	2.08	8.26	10.39	-	0.05	48.24	233.45	189.24	1091.47
	RC15 −2	564.40	2.16	2.08	12.38	10.39	-	0.05	48.24	233.45	189.24	1062.40
	RC20 −2	531.20	2.16	2.08	16.51	10.39	-	0.05	48.24	233.45	189.24	1033.32
B4	RS5-CP10 −2	664.00	2.05	2.08	0.79	9.35	4.7	0.05	48.24	233.45	189.24	1153.93
	RS5-CP15 −2	664.00	2.05	2.08	0.79	8.83	7.0	0.05	48.24	233.45	189.24	1155.75
	RS5-CP20 −2	664.00	2.05	2.08	0.79	8.31	9.4	0.05	48.24	233.45	189.24	1157.57

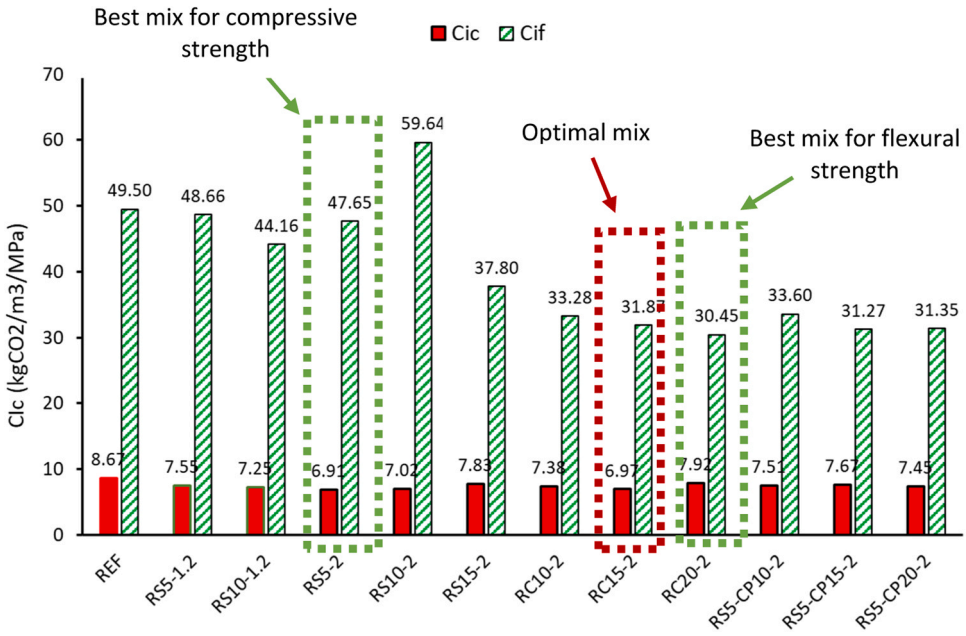

Fig. 14. Compressive and flexural carbon indexes of all mixtures.

Table 8
The cost of the raw materials.

Raw materials	Unit price (AUD/ton)	Reference
Cement	309.00	[42]
SF	1092.00	[42]
FA	833.00	[76]
RHA	22.50*	[74]
SS	328.00	[42]
CP	7.50*	[75]
Water	2.73	[42]
Steel fibre	1564.00	[42]
SP	5460.00	[76]

* The price was converted from USD to AUD using the exchange rate of the reported year.

$$CBR_c = \frac{Production\ Cost\left(\frac{AUD}{m^3}\right)}{Compressive\ strength(MPa)} \quad (5)$$

$$CBR_f = \frac{Production\ Cost\left(\frac{AUD}{m^3}\right)}{Flexural\ strength(MPa)} \quad (6)$$

energy consumption in the production processes. Since the energy usage is mainly influenced by the employed technologies, which have not significantly improved since 2019, the energy consumption is anticipated to change slightly. Thus, material prices are expected to not deviate considerably from the values outlined in Table 8; and the analysis results can still offer a good initial assessment for engineers to choose suitable materials for UHPC mix designs.

Table 9 provides the production costs of UHPC blends. Markedly, developed mixtures possessed marginally lower costs compared to the conventional mix. Since RHA was much less costly than cement and SF, increasing the ratio of RHA replacement induced to lower production costs, by 6.6–7.2 %, 0.6–1.7 %, and 1.6–3.2 % for B1, B2, and B3, respectively. Similarly, as the unit price of CP was much smaller than that of SS, B4′s mixtures also achieved a 2.9–5.2 % cost saving. To simultaneously consider the mixtures' mechanical performance and their production costs, a cost benefit ratio (CBR), computed by the production cost per unit strength (see Eq. (5) and Eq. (6)), was utilised to analyse the economic efficiency of the UHPC mixtures.

Fig. 15 depicts the production cost per unit compressive/flexural strength for all blends. Accordingly, the CBR_c of the control mix was the highest value, at 11 AUD/MPa/m^3. The presence of RHA in the UHPC samples led to enhanced economic efficiency; however, this advantage was not positively proportional to the RHA content. While the CBR_c values of batch B1 dropped from 9.6 to 9.2 AUD/MPa/m^3 with the

Table 9
Production costs of the studied mixtures.

		Compositions									Production cost (AUD/m^3)
		Cement	SF	Fly ash	RHA	SS	CP	Water	SP	Steel fibre	
REF		247.20	168.17	64.22	0	340.66	0	0.49	365.82	243.98	1452.22
B1	RS5 −1.2	247.20	159.76	64.22	0.17	340.66	0	0.49	365.82	156.40	1356.40
	RS10 −1.2	247.20	151.35	64.22	0.35	340.66	0	0.49	365.82	156.40	1348.16
B2	RS5 −2	247.20	159.76	64.22	0.17	340.66	0	0.49	365.82	243.98	1443.98
	RS10 −2	247.20	151.35	64.22	0.35	340.66	0	0.49	365.82	243.98	1435.75
	RS15 −2	247.20	142.94	64.22	0.52	340.66	0	0.49	365.82	243.98	1427.51
B3	RC10 −2	222.48	168.17	64.22	1.80	340.66	0	0.49	365.82	243.98	1429.30
	RC15 −2	210.12	168.17	64.22	2.70	340.66	0	0.49	365.82	243.98	1417.84
	RC20 −2	197.76	168.17	64.22	3.60	340.66	0	0.49	365.82	243.98	1406.38
B4	RS5-CP10 −2	247.20	159.76	64.22	0.17	306.59	0.78	0.49	365.82	243.98	1410.69
	RS5-CP15 −2	247.20	159.76	64.22	0.17	289.56	1.17	0.49	365.82	243.98	1394.05
	RS5-CP20 −2	247.20	159.76	64.22	0.17	272.53	1.56	0.49	365.82	243.98	1377.41

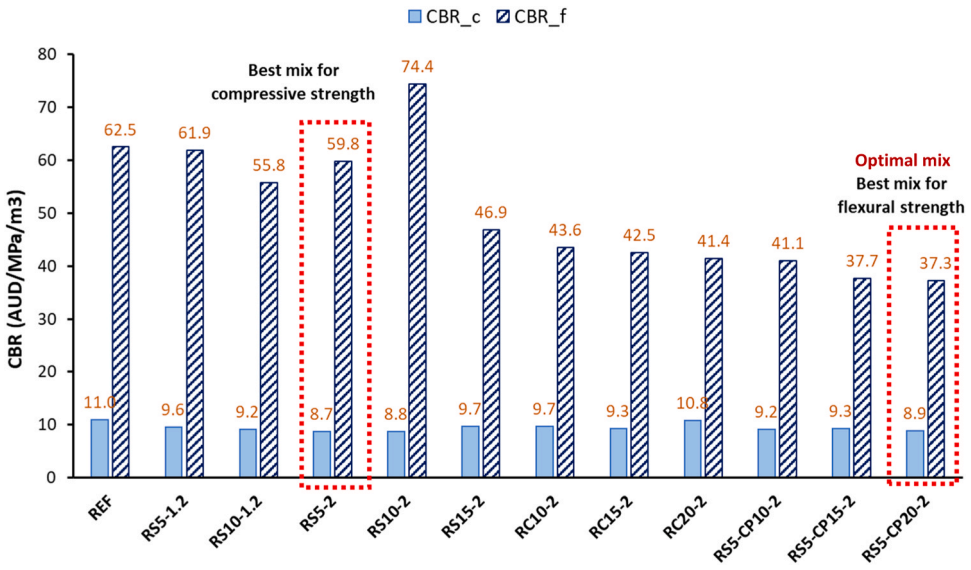

Fig. 15. Cost benefit ratios of the tested mixtures.

increase in RHA proportion, this reduction was not obvious for other batches. Except for RS15–2, Batch B2 obtained the largest cost efficiency of about 21 % with up to 10 % RHA. Likewise, positive outcomes were achieved for CP-added mixtures, with a maximum reduction of 19.1 %. Noticeably, mixtures that partially replaced cement with RHA (batch B3) were generally less economical than those substituting RHA for SF (batches B1 and B2). This could be explained by the much worse compressive resistance and moderate cost savings when substituting RHA for cement in batch B3.

While the CBR_c figures did not demonstrate a clear downward trend with the rise in RHA substitution dosage, the CBR_f counterparts were consistently and negatively related with the RHA content. From Fig. 15, it was explicit that the cost efficiency of the UHPCs was greatly enhanced when replacing RHA with cement. Accordingly, cost savings of 4.4–25.1 % and 30.3–33.7 % were respectively obtained for batches B2 and B3. Due to their greatly improved flexural resistance and the much lower price of CP compared to SS, B4′s mixtures demonstrated substantial improvements in economic efficiency (up to 40 % cost reduction).

In brief, the studied UHPCs generally exhibited greater economic efficiency than the conventional mixture. While RS5–2 proved to be the most economical mixture considering compressive resistance, RS5-CP20–2 was the cheapest mix for flexural strength. Notably, RS5-CP20–2 also stood out as the overall optimal mixture, maintaining both acceptably low compressive and flexural cost indexes. These findings consistently underscore the advantageous combined effects of RHA and CP in producing cost-effective UHPCs without compromising its technical performance.

6. Conclusion

This research investigated the effects of pozzolanic RHA and CP on the mechanical and damping properties of UHPCs. The following conclusions have been drawn from the results presented in this study:

- The addition of RHA and CP in mixtures reduced the workability of UHPCs, especially when replacing cement by RHA.
- Without CP, RHA-based UHPCs exhibited either higher or comparable compressive strengths to the control mix, with up to 15 % RHA content. The dual presence of RHA and CP in mixtures resulted in a 13.6-17.2 % increase in their compressive resistance, indicating the advantageous synthetic effect of RHA and CP addition.
- While substituting SF by RHA could lead to a 4-31.2 % rise in flexural strengths, partially replacing cement with RHA greatly improved the flexural capacity, by 41.2-46.1 %. With the inclusion of RHA and CP, mixtures' bending capacity was further boosted by 47.9-59.1 %.
- The presence of RHA in the concrete mixes improved their damping ratios, reaching a maximum enhancement of 68 % with 15 % RHA substitution. Moreover, an optimal amount of RHA replacement level and steel fibres could augment the damping property of UHPC mixtures.
- Considering technical, environmental, and economic aspects altogether, developed mixtures outperformed the conventional UHPC. While the best substituting dosage of RHA for SF cannot be concluded, the optimal replacement proportions of RHA for cement and CP for SS were found at 20 %.

In conclusion, this study demonstrated the feasibility and benefits of utilising the industrial waste materials RHA and CP as supplementary cementitious materials for producing sustainable and high-performance UHPC. The synergistic combination of RHA and CP not only enhanced the mechanical properties, including compressive strength, flexural strength, and damping ratio, but also reduced the environmental impact and production cost compared to conventional UHPC. The optimal replacement levels were found to be 5–10 % RHA for SF, 20 % RHA for cement, and up to 20 % CP for silica sand. These findings added another option for the development of eco-friendly and cost-effective UHPC mixtures by valorising locally available waste materials, contributing to a more sustainable construction industry.

CRediT authorship contribution statement

Tung Minh Tran: Writing – review & editing. **Paththini HHU Fernando:** Methodology, Investigation, Formal analysis, Data curation. **Hoang TMK Trinh:** Writing – original draft, Methodology, Investigation, Formal analysis. **Thong Pham:** Writing – review & editing, Supervision, Project administration, Methodology, Funding acquisition, Conceptualization.

Declaration of Competing Interest

The authors have no relevant financial or non-financial interests to disclose.

Acknowledgement

The authors acknowledge the financial support from Australian Research Council (ARC) Grant number DP220100307. The technical support during the course of this experiment at Curtin University is greatly appreciated.

References

[1] Richard P, Cheyrezy MH. Reactive powder concretes with high ductility and 200-800 MPa compressive strength 1994;144:507–18.
[2] Richard P, Cheyrezy M. Composition of reactive powder concretes. Cem Concr Res 1995;25(7):1501–11.
[3] Nguyen VT, Ye G, van Breugel K, Fraaij ALA, Bui DD. The study of using rice husk ash to produce ultra high performance concrete. Constr Build Mater 2011;25(4):2030–5.
[4] S.-J. Kwon X.-Y. Wang Optimization of the mixture design of low-CO2 high-strength concrete containing silica fume 2019.
[5] Soliman NA, Tagnit-Hamou A. Partial substitution of silica fume with fine glass powder in UHPC: filling the micro gap. Constr Build Mater 2017;139:374–83. /05/15/ 2017.
[6] Bahedh MA, Jaafar MS. Ultra high-performance concrete utilizing fly ash as cement replacement under autoclaving technique. Case Stud Constr Mater 2018;9:e00202. /12/01/ 2018.
[7] Teng S, Lim TYD, Sabet Divsholi B. Durability and mechanical properties of high strength concrete incorporating ultra fine Ground Granulated Blast-furnace Slag. Constr Build Mater 2013;40:875–81. /03/01/ 2013.
[8] Wu Z, Khayat KH, Shi C. Changes in rheology and mechanical properties of ultra-high performance concrete with silica fume content. Cem Concr Res 2019;123:105786. /09/01/ 2019.
[9] Kalakada Z, Doh JH, Zi G. Utilisation of coarse glass powder as pozzolanic cement—a mix design investigation. Constr Build Mater 2020;vol. 240:117916.
[10] Mosaberpanah MA, Umar SA. Utilizing rice husk ash as supplement to cementitious materials on performance of ultra high performance concrete: – a review. Mate Today Sustain 2020;7-8:100030.
[11] Thomas BS. Green concrete partially comprised of rice husk ash as a supplementary cementitious material – a comprehensive review. Renew Sustain Energy Rev 2018;82:3913–23.
[12] Alkhaly YR, Husaini Abdullah, Hasan M. Characteristics of reactive powder concrete comprising synthesized rice husk ash and quartzite powder. J Clean Prod 2022;375:134154.
[13] Vigneshwari M, Arunachalam K, Angayarkanni A. Replacement of silica fume with thermally treated rice husk ash in reactive powder concrete. J Clean Prod 2018;188:264–77. /07/01/ 2018.
[14] Zhang MH, Lastra R, Malhotra VM. Rice-husk ash paste and concrete: Some aspects of hydration and the microstructure of the interfacial zone between the aggregate and paste. Cem Concr Res 1996;26(6):963–77. /06/01/ 1996.
[15] Salas A, Delvasto S, de Gutierrez RM, Lange D. Comparison of two processes for treating rice husk ash for use in high performance concrete. Cem Concr Res 2009;39(9):773–8. /09/01/ 2009.
[16] Kang S-H, Hong S-G, Moon J. The use of rice husk ash as reactive filler in ultra-high performance concrete. Cem Concr Res 2019;115:389–400. /01/01/ 2019.
[17] Huang H, Gao X, Wang H, Ye H. Influence of rice husk ash on strength and permeability of ultra-high performance concrete. Constr Build Mater 2017;149:621–8. /09/15/ 2017.
[18] Nguyen VT, Ye G, van Breugel K, Copuroglu O. Hydration and microstructure of ultra high performance concrete incorporating rice husk ash. Cem Concr Res 2011;41(11):1104–11.
[19] Chao-Lung H, Anh-Tuan BL, Chun-Tsun C. Effect of rice husk ash on the strength and durability characteristics of concrete. Constr Build Mater 2011;25(9):3768–72.
[20] Chindaprasirt P, Homwuttiwong S, Jaturapitakkul C. Strength and water permeability of concrete containing palm oil fuel ash and rice husk–bark ash. Constr Build Mater 2007;21(7):1492–9.
[21] Gastaldini ALG, Isaia GC, Gomes NS, Sperb JEK. Chloride penetration and carbonation in concrete with rice husk ash and chemical activators. Cem Concr Compos 2007;29(3):176–80. /03/01/ 2007.
[22] Saraswathy V, Song H-W. Corrosion performance of rice husk ash blended concrete. Constr Build Mater 2007;21(8):1779–84.
[23] Cordeiro GC, Toledo Filho RD, de Moraes Rego Fairbairn E. Use of ultrafine rice husk ash with high-carbon content as pozzolan in high performance concrete. Mater Struct 2009;42(7):983–92. /08/01 2009.
[24] Safiuddin M, West JS, Soudki KA. Hardened properties of self-consolidating high performance concrete including rice husk ash. Cem Concr Compos 2010;32(9):708–17. /10/01/ 2010.
[25] Van V-T-A, Rößler C, Bui D-D, Ludwig H-M. Rice husk ash as both pozzolanic admixture and internal curing agent in ultra-high performance concrete. Cem Concr Compos 2014;53:270–8. /10/01/ 2014.
[26] Ray S, Haque M, Sakib MN, Mita AF, Rahman MDM, Tanmoy BB. Use of ceramic wastes as aggregates in concrete production: a review. J Build Eng 2021;43:102567.
[27] Mukhopadhyay TK, Ghosh S, Ghatak S. Phase analysis and microstructure evolution of a bone china body modified with scrap addition. Ceram Int 2011;37(5):1615–23.
[28] Halicka A, Ogrodnik P, Zegardlo B. Using ceramic sanitary ware waste as concrete aggregate. Constr Build Mater 2013;48:295–305. /11/01/ 2013.
[29] Medina C, Sánchez de Rojas MI, Frías M. Reuse of sanitary ceramic wastes as coarse aggregate in eco-efficient concretes. Cem Concr Compos 2012;34(1):48–54. /01/01/ 2012.
[30] Canbaz M. The effect of high temperature on concrete with waste ceramic aggregate. Iran J Sci Technol, Trans Civ Eng 2016;40(1):41–8. /03/01 2016.
[31] Guerra I, Vivar I, Llamas B, Juan A, Moran J. Eco-efficient concretes: the effects of using recycled ceramic material from sanitary installations on the mechanical properties of concrete. Waste Manag 2009;29(2):643–6. /02/01/ 2009.
[32] Zegardło B, Szeląg M, Ogrodnik P. Ultra-high strength concrete made with recycled aggregate from sanitary ceramic wastes – the method of production and the interfacial transition zone. Constr Build Mater 2016;122:736–42. /09/30/ 2016.
[33] Kannan DM, Aboubakr SH, El-Dieb AS, Reda Taha MM. High performance concrete incorporating ceramic waste powder as large partial replacement of Portland cement. Constr Build Mater 2017;144:35–41. /07/30/ 2017.
[34] Xu K, et al. Mechanical properties of low-carbon ultrahigh-performance concrete with ceramic tile waste powder. Constr Build Mater 2021;vol. 287:123036.
[35] AS 3972–2010 – General purpose and blended cements, 2010.
[36] Yu R, Spiesz P, Brouwers HJH. Static properties and impact resistance of a green ultra-high performance hybrid fibre reinforced concrete (UHPHFRC): experiments and modeling. Constr Build Mater 2014;68:158–71. /10/15/ 2014.
[37] Alyami M, Hakeem IY, Amin M, Zeyad AM, Tayeh BA, Agwa IS. Effect of agricultural olive, rice husk and sugarcane leaf waste ashes on sustainable ultra-high-performance concrete. J Build Eng 2023;72:106689.
[38] Ha NS, Marundrury SS, Pham TM, Pournasiri E, Shi F, Hao H. Effect of grounded blast furnace slag and rice husk ash on performance of ultra-high-performance concrete (UHPC) subjected to impact loading. Constr Build Mater 2022;329:127213.
[39] AS 1012.2:2014 - Methods of testing concrete. Method 2: Preparing concrete mixes in the laboratory, 2014.
[40] AS 1012.8.1:2014 - Methods of testing concrete. Method for making and curing concrete - Compression and indirect tensile test specimens., 2014.
[41] AS 1012.3.5:2015 - Methods of testing concrete. Determination of properties related to the consistency of concrete - Slump flow, T500 and J-ring test, 2015.
[42] Isa MN, Pilakoutas K, Guadagnini M, Angelakopoulos H. Mechanical performance of affordable and eco-efficient ultra-high performance concrete (UHPC) containing recycled tyre steel fibres. Constr Build Mater 2020;255:119272.
[43] Wu Z, Shi C, He W, Wu L. Effects of steel fiber content and shape on mechanical properties of ultra high performance concrete. Constr Build Mater 2016;103:8–14. /01/30/ 2016.
[44] ASTM C109/C109M-13 – Standard test method for compressive strength of hydraulic cement mortars, 2021.
[45] ASTM E756–05 – Measuring vibration-damping properties of materials, 2017.
[46] ASTM C78/C78M-22 – Standard test method for flexural strength of concrete, 2022.
[47] Varadharajan S, Jaiswal A, Verma S. Assessment of mechanical properties and environmental benefits of using rice husk ash and marble dust in concrete. Structures 2020;28:389–406. /12/01/ 2020.
[48] Celik F, Canakci H. An investigation of rheological properties of cement-based grout mixed with rice husk ash (RHA). Constr Build Mater 2015;91:187–94. /08/30/ 2015.
[49] Şahmaran M, Christianto HA, Yaman İÖ. The effect of chemical admixtures and mineral additives on the properties of self-compacting mortars. Cem Concr Compos 2006;28(5):432–40.
[50] Yahia A, Tanimura M, Shimoyama Y. Rheological properties of highly flowable mortar containing limestone filler-effect of powder content and W/C ratio. Cem Concr Res 2005;35(3):532–9. /03/01/ 2005.
[51] Gomes M, de Brito J. Structural concrete with incorporation of coarse recycled concrete and ceramic aggregates: durability performance. Mater Struct 2009;42(5):663–75. /06/01 2009.
[52] El-Abbasy AA. Production, behaviour and mechanical properties of ultra-high-performance fiber concrete – a comprehensive review. Case Stud Constr Mater 2022;17:e01637. /12/01/ 2022.
[53] Bie R-S, Song X-F, Liu Q-Q, Ji X-Y, Chen P. Studies on effects of burning conditions and rice husk ash (RHA) blending amount on the mechanical behavior of cement. Cem Concr Compos 2015;55:162–8. /01/01/ 2015.
[54] Chopra D, Siddique R, Kunal. Strength, permeability and microstructure of self-compacting concrete containing rice husk ash. Biosyst Eng 2015;130:72–80. /02/01/ 2015.
[55] Kannan V, Ganesan K. Chloride and chemical resistance of self compacting concrete containing rice husk ash and metakaolin. Constr Build Mater 2014;51:225–34. /01/31/ 2014.
[56] He Z-h, Li L-y, Du S-g. Creep analysis of concrete containing rice husk ash. Cem Concr Compos 2017;80:190–9. /07/01/ 2017.
[57] Siddesha H. Experimental studies on the effect of ceramic fine aggregate on the strength properties of concrete. Int J Eng, Sci Technol 2011;1(1):71–6.
[58] Wei J, Meyer C. Utilization of rice husk ash in green natural fiber-reinforced cement composites: Mitigating degradation of sisal fiber. Cem Concr Res 2016;vol. 81:94–111. /03/01/ 2016.
[59] Safdar Raza S, Ali B, Noman M, Fahad M, Mohamed Elhadi K. Mechanical properties, flexural behavior, and chloride permeability of high-performance steel fiber-reinforced concrete (SFRC) modified with rice husk ash and micro-silica. Constr Build Mater 2022;359:129520.
[60] Bixapathi G, Saravanan M. Strength and durability of concrete using Rice Husk ash as a partial replacement of cement. Mater Today: Proc 2022;52:1606–10.

[61] Ameri F, Shoaei P, Bahrami N, Vaezi M, Ozbakkaloglu T. Optimum rice husk ash content and bacterial concentration in self-compacting concrete. Constr Build Mater 2019;222:796–813. /10/20/ 2019.
[62] Tayeh BA, Alyousef R, Alabduljabbar H, Alaskar A. Recycling of rice husk waste for a sustainable concrete: a critical review. J Clean Prod 2021;312:127734.
[63] Johnson Daniel R, Sangeetha SP. Experimental study on concrete using waste ceramic as partial replacement of aggregate. Mater Today: Proc 2021;45:6603–8.
[64] Lee KS, Choi J-I, Kim S-K, Lee B-K, Hwang J-S, Lee BY. Damping and mechanical properties of composite composed of polyurethane matrix and preplaced aggregates. Constr Build Mater 2017;145:68–75. /08/01/ 2017.
[65] Papageorgiou AV, Gantes CJ. Equivalent modal damping ratios for concrete/steel mixed structures. Comput Struct 2010;88(19):1124–36.
[66] Bernal D, Döhler M, Kojidi SM, Kwan K, Liu Y. First mode damping ratios for buildings. Earthq Spectra 2015;31(1):367–81. /02/01 2015.
[67] Dai K, Lu D, Zhang S, Shi Y, Meng J, Huang Z. Study on the damping ratios of reinforced concrete structures from seismic response records. Eng Struct 2020;223:111143.
[68] xi Y, Wenhua Z, Yilin P, wanting Z, Fenghao Y. Comparative study on damping test methods of concrete materials. Constr Build Mater 2021;300:124367.
[69] Turner LK, Collins FG. Carbon dioxide equivalent (CO_2-e) emissions: a comparison between geopolymer and OPC cement concrete. Constr Build Mater 2013;43:125–30. /06/01/ 2013.
[70] D.G. Miller and E. Griffith University. Griffith School of, "Incorporating environmentally efficient structural engineering design into concrete buildings," Dissertation/Thesis, 2015.
[71] Shi Y, Long G, Ma C, Xie Y, He J. Design and preparation of ultra-high performance concrete with low environmental impact. J Clean Prod 2019;214:633–43. /03/20/ 2019.
[72] Park S, Wu S, Liu Z, Pyo S. The role of supplementary cementitious materials (SCMs) in ultra high performance concrete (UHPC): a review. no 2021;14(6):1472.
[73] Samadi M, et al. Waste ceramic as low cost and eco-friendly materials in the production of sustainable mortars. J Clean Prod 2020;266:121825.
[74] Ozturk E, Ince C, Derogar S, Ball R. Factors affecting the CO_2 emissions, cost efficiency and eco-strength efficiency of concrete containing rice husk ash: a database study. Constr Build Mater 2022;326:126905.
[75] Abd Ellatief M, Abadel AA, Federowicz K, Abd Elrahman M. Mechanical properties, high temperature resistance and microstructure of eco-friendly ultra-high performance geopolymer concrete: role of ceramic waste addition. Constr Build Mater 2023;401:132677.
[76] Nguyen T-T, Thai H-T, Ngo T. Optimised mix design and elastic modulus prediction of ultra-high strength concrete. Constr Build Mater 2021;302:124150.